

Self-Healing Ability of Poly(PEGMA-5-UPy) Evaluated by Thermomechanical Analysis

Elisa Calabrese,* Liberata Guadagno, Marialuigia Raimondo, Andrea Sorrentino,*
Simona Russo,* Pasquale Longo, and Annaluisa Mariconda

The synthesis and characterization of polyethylene glycol monomethyl ether methacrylate (PEGMA) based copolymers incorporating three different percentages (2.5 wt%, 5.0 wt%, and 7.8 wt%) of urea-*N*-2-amino-4-hydroxy-6-methylpyrimidine-*N'*-(hexametylen-*n*-carboxyethyl methacrylate) (HEMA-UPy) are reported. Nuclear magnetic resonance (NMR) and infrared spectroscopy (IR) confirm the synthesis procedure. Differential scanning calorimetry (DSC) and thermogravimetric analysis (TGA) are employed to evaluate the thermal properties of the samples. DSC measurements evidence a slight increase in glass transition temperature (T_g), a consistent increase in crystallization and melting temperatures (T_c and T_m), and a reduction in the crystallization degree (X_c) with increasing the amount of HEMA-UPy moiety. Dynamic mechanical analysis (DMA) is carried out at different values of temperature and oscillation frequency. It highlights the ability of the healed copolymer to recover the pristine values of storage modulus. The healing efficiency depends on the temperature history of the sample. For the sample healed at room temperature, the value of healing efficiency is 64%. DMA tests performed at higher temperatures, after some permanence at room temperature, evidence higher values in the healing efficiency. This demonstrates that the higher value of the temperature employed during DMA tests determines greater mobility of the chains causing an enhancement in the healing efficiency.

safety, extended service life, lower costs in service, and reduced environmental impact.^[1–3]

Self-healing materials manifest the intrinsic ability to the auto-repair, recovering the pristine functionality.^[3] They can be classified as extrinsic and intrinsic auto-regenerating materials. In extrinsic systems, the auto-repair mechanism is triggered by the polymerization reaction of a self-healing agent stored in microcapsules or vascular networks.^[4–11] In particular, in the case of micro-encapsulated systems, relevant results have been achieved by the synthesis of a new catalyst suitable to fulfill the needs of structural materials and capable of overcoming criticalities related to the temperature used in the processing of industrial resins designed to withstand high aerodynamic loads.^[12–14] Furthermore, significant advances have also been made in the microstructural characterization of the microcapsules through micro-computed tomography (μ CT). This method was used to investigate the dimensional distribution of the microcapsules in a polymer system with self-healing properties.^[15]

Intrinsic self-healing materials generally are based on reversible bonds.^[16] For example, self-healing intrinsic polymeric materials based on reversible covalent reactions, such as Diels–Alder and retro Diels–Alder or disulfide exchange reactions, have been developed.^[17] Concerning Diels–Alder materials, the

1. Introduction


Biological systems and their spontaneous self-generating capacity have been a source of inspiration for the development of self-healing materials, characterized by enormous advantages such as

E. Calabrese, L. Guadagno, M. Raimondo
Department of Industrial Engineering
University of Salerno
Via Giovanni Paolo II, Fisciano, Salerno 84084, Italy
E-mail: elicalabrese@unisa.it

A. Sorrentino
Institute for Polymers, Composites, and Biomaterials (IPCB-CNR)
via Previati n. 1/E, Lecco 23900, Italy
E-mail: andrea.sorrentino@cnr.it

S. Russo, P. Longo
Department of Chemistry and Biology
University of Salerno
Via Giovanni Paolo II, 132, Fisciano, Salerno 84084, Italy
E-mail: sirusso@unisa.it

A. Mariconda
Department of Science
University of Basilicata
Viale dell'Ateneo Lucano, 10, Potenza 85100, Italy

 The ORCID identification number(s) for the author(s) of this article can be found under <https://doi.org/10.1002/mame.202200500>

© 2022 The Authors. Macromolecular Materials and Engineering published by Wiley-VCH GmbH. This is an open access article under the terms of the Creative Commons Attribution License, which permits use, distribution and reproduction in any medium, provided the original work is properly cited.

DOI: 10.1002/mame.202200500

auto-repair mechanism can be thermally activated or they can heal at ambient temperature.^[18–29] For ionic copolymers, the formation of clusters, which act as reversible crosslinks, can be triggered by temperature or ultraviolet irradiation (UV). For supramolecular elastomeric polymers, based on non-covalent hydrogen bonding interactions, the self-repair is mechanically activated by bringing back in contact the damaged pieces, allowing the restoration of the reversible bonds at ambient temperature.^[30–35] Furthermore, the intrinsic self-healing materials must be characterized by mechanical properties suitable for their intended applications. For structural materials, high mechanical performance is required.

With the purpose of obtaining structural self-responsive composites, various winning approaches have been developed, such as those based on the use of carbon nanofillers embedded in a toughened epoxy matrix.^[36–49]

Concerning thermoplastic materials, several composites showing self-healing ability at ambient temperature have been proposed. Among these, a commercial biodegradable polymer with high gas barrier properties is worth mentioning.^[50–56] This polymer has been made electrically conductive through the use of carbon nano-particles dispersed in the matrix using ionic liquids (ILs) or by mixing it with a highly compatible masterbatch based on carboxymethyl cellulose (CMC). In this last case, the self-repair ability has been conferred to the material by adding a molecule capable of acting as a healing agent.^[48,57–61]

In recent years, an important step forward in supramolecular chemistry has been possible thanks to the work of Beijer et al., with the synthesis of the ureidopyrimidinone (UPy) dimer, that, due to its high dimerization constant, is considered “the novel building-block for self-assembly.”^[62] Since then, UPy units, combined with several elastomeric matrices such as poly(butyl acrylate) (PBA) and poly(ethylene glycol) (PEG), have been employed to formulate self-healing copolymers, whose adhesion properties have been investigated to develop biocompatible materials, having potential application in tissue engineering or for obtaining flexible electronic devices.^[63–66]

Herein the authors, inspired by the research work of Chen et al., have prepared the supramolecular elastomer poly(polyethylene glycol monomethyl ether methacrylate-co-HEMA-UPy) (Poly (PEGMA-co-UPy)), by incorporating three different percentages of HEMA-UPy unit (2.5 wt%, 5.0 wt%, and 7.8 wt%), to accurately investigate the thermal properties and the self-healing ability of the formulated materials.^[66] In particular, in this work, the authors use TGA and DSC investigations as diagnostic methods to demonstrate the presence of hydrogen bonding interactions and to show how these bonds affect the thermal transitions and the thermal stability of the samples. Furthermore, they propose a new method to evaluate self-healing ability of Poly (PEGMA-5-UPy) copolymer, based on DMA measurements.

Through this work, the authors wish to contribute further to studying these materials having high potential for futuristic, intelligent applications, such as sensing applications or new electronic soft devices.^[65,66] Furthermore, it has been found that conductive nanoparticles dispersed in the polymeric matrix allow conferring of many self-responsive properties to the hosting polymeric matrix, among them: self-sensing, de-icing, and so on.^[36] The possible dispersion of conductive nanoparticles in the developed polymer would pave the way for the development

of smart self-healing materials in the form of bulk or coating materials.

2. Experimental Section

2.1. Materials

All reagents were bought by Merck or TCI Chemicals. 2-amino-4-hydroxy-6-methylpyrimidine (>98%, TCI), hexamethylene diisocyanate (>98%, TCI), polyethylene glycol monomethyl ether methacrylate stabilized with MEHQ (PEGMA, Mw = 500, TCI), dibutyltin dilaurate (>95%, TCI), and 2-2'-azobis(2-methylpropionitrile) (AIBN, 98%, Merck) were used as received, whereas 2-hydroxyethyl methacrylate stabilized with MEHQ (HEMA, >95%, TCI) was distilled before use. *N,N*-Dimethylformamide (DMF) and chloroform solvents were used without further purification. All reactions were performed under nitrogen atmosphere using standard Schlenk and glovebox techniques.

2.1.1. Synthesis of 2-(6-Isocyanatohexylaminocarbonylamino)-6-methyl-4[1H]pyrimidinone OCN-UPy

2-Amino-4-hydroxy-6-methylpyrimidine (2.00 g, 16 mmol) and an excess of hexamethylene diisocyanate (16.2 g, 96.3 mmol) were introduced in a 50 mL glass-flask, which was kept at 100 °C for 20 h under nitrogen atmosphere. The reaction mixture was transferred to another flask and then washed with 4 × 100 mL of pentane, in order to eliminate the excess of hexamethylene diisocyanate. The product was recovered by filtration as a white solid. Yield: 75%.

The detailed synthesis reaction is depicted in **Figure 1a**.

¹H NMR (300 MHz, CDCl₃, 298 K, δ): 13.1 (s, 1H, CH₃CNH), 11.9 (s, 1H, CH₂NH(C=O)NH), 10.2 (s, 1H, CH₂NH(C=O)NH), 5.80 (s, 1H, CH₃C=CH), 3.30 (m, *J* = 6.46 Hz, 4H; OCNCH₂, CH₂NH(C=O)NH), 2.20 (s, 3H, CH₃C=CH), 1.60 (m, *J* = 8.07 Hz, 4H; OCNCH₂CH₂, CH₂CH₂NH(C=O)NH), 1.40 (m, *J* = 6.06 Hz, 4H; CH₂CH₂CH₂CH₂CH₂CH₂).

¹³C NMR (100 MHz, CDCl₃, 298 K, δ): 173.3 (NC=OCH), 156.8 (CH₃C=CH), 154.9 (N(C=O)N), 148.5 (NHC=N), 122.0 (O=CN), 106.9 (CH₃C=CH), 43.1 (OCNCH₂), 40.0 (CH₂NH(C=O)NH), 31.4 (OCNCH₂CH₂), 29.5 (CH₂CH₂NH(C=O)NH), 26.4 (CH₂CH₂CH₂CH₂CH₂CH₂), 19.2 (CH₃C=CH).

2.1.2. Synthesis of Urea-N-2-amino-4-hydroxy-6-methylpyrimidine-N'-(hexametylen-N-carboxyethyl methacrylate) HEMA-UPY

The freshly synthesized OCN-UPy (4.35 g, 14.7 mmol) was transferred into a two-necked 250 mL flask with distilled 2-hydroxyethyl methacrylate HEMA (3.86 g, 29.6 mmol) and dibutyltin dilaurate (one drop) in 120 mL of chloroform as solvent. The blend was mixed at 60 °C for 20 h under nitrogen atmosphere. At the end of the reaction, the mixture was filtered through a Büchner funnel. The solution was concentrated and diethyl ether was added, obtaining the precipitation of the product,

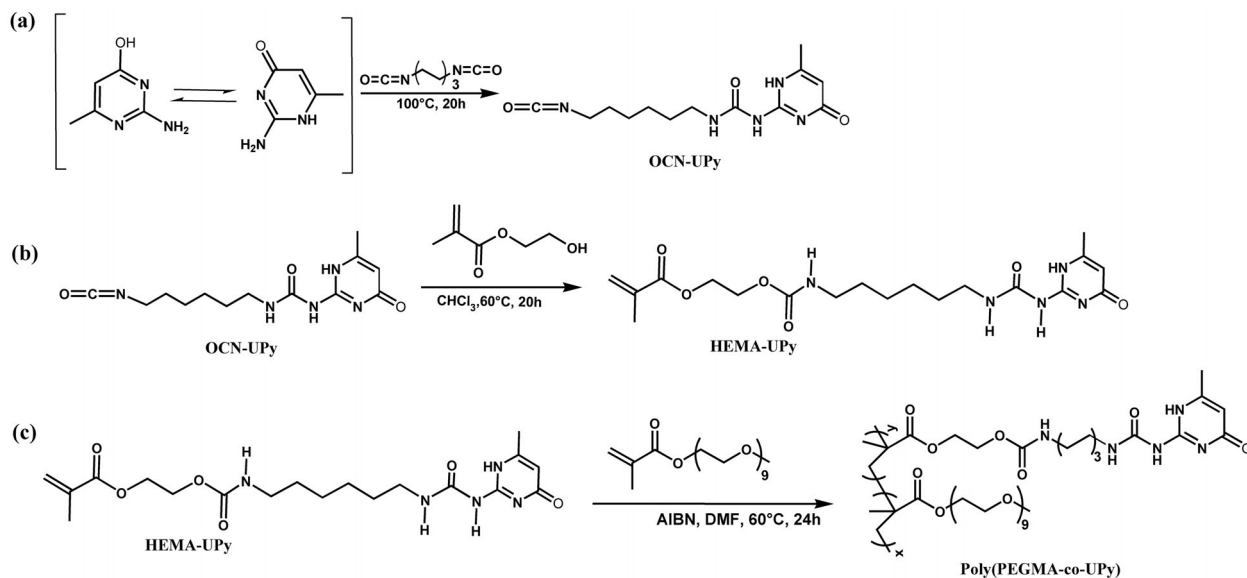


Figure 1. Synthesis procedure of copolymers Poly(PEGMA-co-UPy). a) Synthesis of OCN-UPy. b) Synthesis of HEMA-UPy. c) Synthesis of Poly(PEGMA-co-UPy).

which was recovered by filtration and dried in the oven overnight. The synthesis procedure is shown in Figure 1b. Yield: 80%.

^1H NMR (300 MHz, CDCl_3 , 298 K, δ): 13.2 (s, 1H, CH_3CNH), 11.9 (s, 1H, $\text{CH}_2\text{NH}(\text{C}=\text{O})\text{NH}$), 10.2 (s, 1H, $\text{CH}_2\text{NH}(\text{C}=\text{O})\text{NH}$), 6.10 + 5.60 (d, $J = 1.45$ Hz, 2H; $\text{C}=\text{CH}_2$), 5.80 (s, 1H, $\text{CH}_3\text{C}=\text{CH}$), 5.00 (m, 1H, $\text{O}(\text{C}=\text{O})\text{NH}$), 4.30 (m, $J = 7.84$ Hz, 4H; $\text{O}=\text{COCH}_2\text{CH}_2\text{OC}=\text{O}$), 3.20 (m, $J = 6.44$ Hz, 4H; $\text{O}(\text{C}=\text{O})\text{NHCH}_2$, $\text{CH}_2\text{NH}(\text{C}=\text{O})\text{NH}$); 2.20 (s, 3H, $\text{CH}_3\text{C}=\text{CH}$); 1.90 (s, 3H, $\text{CH}_3\text{C}(\text{C}=\text{O})$), 1.60 (m, $J = 8.05$ Hz, 4H; $\text{OCNCH}_2\text{CH}_2$, $\text{CH}_2\text{CH}_2\text{NH}(\text{C}=\text{O})\text{NH}$), 1.40 (m, $J = 6.34$ Hz, 4H; $\text{CH}_2\text{CH}_2\text{CH}_2\text{CH}_2\text{CH}_2\text{CH}_2$).

^{13}C NMR (150 MHz, CDCl_3 , 298 K, δ): 173.3 ($\text{NC}=\text{OCH}$), 167.3 ($\text{O}=\text{COCH}_2\text{CH}_2\text{OC}=\text{O}$), 156.7 ($\text{O}=\text{COCH}_2\text{CH}_2\text{OC}=\text{O}$), 156.3 ($\text{CH}_3\text{C}=\text{CH}$), 154.9 ($\text{N}(\text{C}=\text{O})\text{N}$), 148.5 ($\text{NHC}=\text{N}$), 136.2 ($\text{C}=\text{CH}_2$), 126.1 ($\text{C}=\text{CH}_2$), 106.8 ($\text{CH}_3\text{C}=\text{CH}$), 63.2 + 62.5 ($\text{O}=\text{COCH}_2\text{CH}_2\text{OC}=\text{O}$), 40.9 + 39.8 ($\text{O}=\text{CNHCH}_2$, $\text{CH}_2\text{NHC}=\text{O}$), 29.8 + 29.5 ($\text{O}=\text{CNHCH}_2\text{CH}_2$, $\text{CH}_2\text{CH}_2\text{NHC}=\text{O}$), 26.4 + 26.2 ($\text{O}=\text{CNHCH}_2\text{CH}_2\text{CH}_2$, $\text{CH}_2\text{CH}_2\text{CH}_2\text{NHC}=\text{O}$), 19.1 ($\text{CH}_3\text{C}=\text{CH}$), 18.4 ($\text{CH}_3\text{C}=\text{CH}_2$).

2.1.3. Synthesis of the Homo Poly(polyethylene glycol monomethyl ether methacrylate)

The homopolymer was synthesized into a two necked 100 mL flask by reaction of polyethylene glycol monomethyl ether methacrylate PEGMA (12 g, 24 mmol) with 2,2'-azobis(2-methylpropanitrile) AIBN (50.0 mg, 0.30 mmol) in *N,N*-dimethylformamide (40 mL). The blend was mixed at 60 °C for 24 h. The solvent was eliminated by a vacuum pump. Yield: 80%.

^1H NMR (300 MHz, TCDE, 353 K, δ): 3.89 (m, 36H, $(\text{C}=\text{O})\text{O}(\text{CH}_2\text{CH}_2\text{O})_9\text{CH}_3$), 3.14 (s, 3H, $(\text{C}=\text{O})\text{O}(\text{CH}_2\text{CH}_2\text{O})_9\text{CH}_3$), 1.65 (b, 2H, CH_2CCH_3), 0.77 (b, 3H, CH_2CCH_3).

^{13}C NMR (150 MHz, TCDE, 353K, δ): 175.1 ($(\text{C}=\text{O})\text{O}(\text{CH}_2\text{CH}_2\text{O})_9\text{CH}_3$), 70.2 + 68.7 + 68.6 + 66.7 + 62.0

($(\text{C}=\text{O})\text{O}(\text{CH}_2\text{CH}_2\text{O})_9\text{CH}_3$), 56.9 ($(\text{C}=\text{O})\text{O}(\text{CH}_2\text{CH}_2\text{O})_9\text{CH}_3$), 43.6 (CH_2CCH_3), 27.82 (CH_2CCH_3), 15.7 (CH_2CCH_3).

2.1.4. Synthesis of Poly(polyethylene glycol monomethyl ether methacrylate-co-HEMA-Upy)

The copolymers were obtained by reaction of polyethylene glycol monomethyl ether methacrylate PEGMA (11.2 g, 22.4 mmol) with the suitable amount of HEMA-UPy (3 mol% [0.237 g, 0.56 mmol], or 5.0 mol% [0.466 g, 1.1 mmol] or 9 mol% [0.741 g, 1.75 mmol]) and 2,2'-azobis(2-methylpropanitrile) AIBN (50.0 mg, 0.30 mmol) in *N,N*-dimethylformamide (40 mL). The reaction was carried out at 60 °C for 24 h in a two-necked 100 mL flask. The product was retrieved by removing the solvent by a vacuum pump. The synthesis route is depicted in Figure 1c. Yield: 80%.

It is worth noting that, before characterizing the formulated samples, they were kept under vacuum for a week at a temperature of 40 °C.

^1H NMR (400 MHz, TCDE, 353 K, δ): 13.0 (s, 1H, CH_3CNH), 11.8 (s, 1H, $\text{CH}_2\text{NH}(\text{C}=\text{O})\text{NH}$), 10.0 (s, 1H, $\text{CH}_2\text{NH}(\text{C}=\text{O})\text{NH}$), 5.85 (s, 1H, $\text{CH}_3\text{C}=\text{CH}$), 3.63 (m, 36H, $(\text{C}=\text{O})\text{O}(\text{CH}_2\text{CH}_2\text{O})_9\text{CH}_3$), 3.36 (s, 3H, $(\text{C}=\text{O})\text{O}(\text{CH}_2\text{CH}_2\text{O})_9\text{CH}_3$), 1.95 (b, 2H, CH_2CCH_3), 1.04 (m, 3H, CH_2CCH_3).

^{13}C NMR (100 MHz, TCDE, 353 K, δ): 175.1 ($(\text{C}=\text{O})\text{O}(\text{CH}_2\text{CH}_2\text{O})_9\text{CH}_3$), 70.2 + 68.7 + 66.7 + 62.0 ($(\text{C}=\text{O})\text{O}(\text{CH}_2\text{CH}_2\text{O})_9\text{CH}_3$), 59.9 ($(\text{C}=\text{O})\text{O}(\text{CH}_2\text{CH}_2\text{O})_9\text{CH}_3$), 43.7 (CH_2CCH_3), 27.2 (CH_2CCH_3), 15.8 (CH_2CCH_3).

2.2. Techniques

2.2.1. NMR Investigation

Synthetic monomers and copolymers had been characterized by ^1H and ^{13}C NMR spectroscopy. All the technical data about the

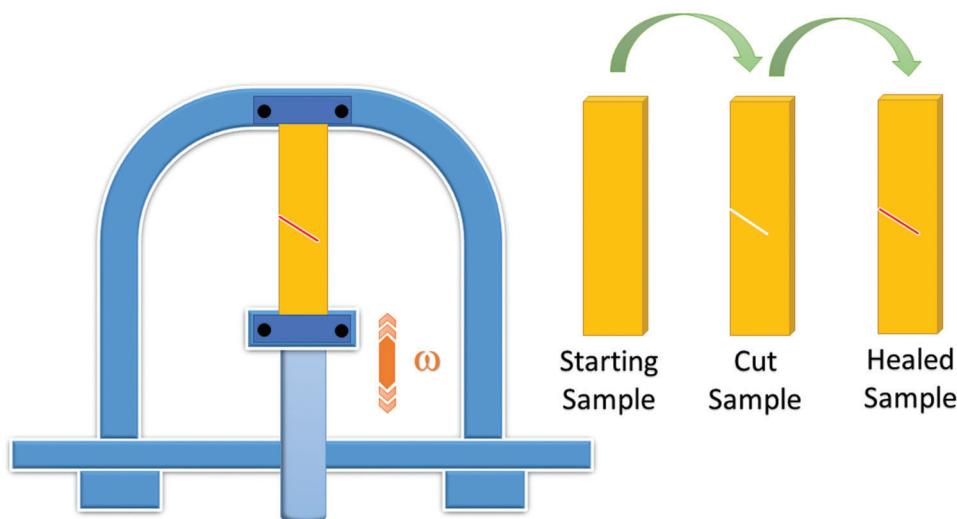


Figure 2. Setup of the DMA tests.

NMR instrumentations have been reported in Section S1, Supporting Information. The samples were formulated by solubilizing about 10 mg of products in 0.5 mL of deuterated solvent (Euriso-Top products). ^1H and ^{13}C chemical shifts are listed in parts per million (ppm) downfield from TMS and are referenced from the solvent peaks or TMS. Spectra have been reported as follows: chemical shift (ppm), multiplicity, and integration. Multiplicities have been abbreviated as follows: singlet (s), doublet (d), triplet (t), multiplet (m), broad (b). Spectra recording and data processing were performed using Bruker-TopSpin v2.1.

2.2.2. Thermal Analysis (TA)

TA of the samples was performed through both DSC and TGA. All the technical data about the DSC and TGA instrumentations have been reported in Section S1, Supporting Information. The DSC measurement was carried out by a single scanning run (rate of $5\text{ }^\circ\text{C min}^{-1}$) from $-90\text{ }^\circ\text{C}$ to $200\text{ }^\circ\text{C}$. The adopted scanning run allowed observation of the glass transition temperature T_g of the formulated copolymers, which showed this parameter at a very low temperature value. T_g was determined by detecting the middle point of the second-order transition of the heating run, while melting temperature T_m and crystallization temperature T_c , were evaluated from the maximum of the endothermic peak and the maximum of the exothermic peak of the heating run, respectively. The crystallinity X_c was determined by using the Equation (1) where ΔH_m^0 is the heat of fusion of pure 100% crystalline of Poly-Ethylene Glycol (PEG) ($\Delta H_m^0 = 196.8\text{ J}\cdot\text{g}^{-1}$) and ΔH_m is the melting heat of the analyzed sample, determined by the evaluation of the total area under the endothermic peak of the heating run.^[67–70]

$$X_c = \frac{\Delta H_m}{\Delta H_m^0} \times 100 \quad (1)$$

Heat of crystallization ΔH_c was evaluated from the calculation of the total area under the exotherm of the heating run.

TGA measurements were carried out in air flow, from $30\text{ }^\circ\text{C}$ to $900\text{ }^\circ\text{C}$, at $10\text{ }^\circ\text{C min}^{-1}$.

2.2.3. Self-Healing Efficiency Evaluation

DMA was adopted to evaluate the self-healing ability of Poly(PEGMA-5-UPy) samples. The tests were performed on specimens with a rectangular geometry ($30 \times 10 \times 0.5\text{ mm}^3$), obtained by using a die-casting technique, through the insertion of the copolymer inside a teflon mold and pressing the sample at $120\text{ }^\circ\text{C}$ for about 3 min. The experimental details adopted for the DMA tests have been reported in Section S1, Supporting Information. Isothermal tests were performed at different oscillation frequencies (1, 10, 30, and 100 Hz) and the constant strain of 0.1%. At each temperature and frequency, virgin and healed samples, before being tested, were left to equilibrate for 5 min. The healed samples were obtained by putting in contact the two surfaces obtained by cutting a virgin sample in half-length at $\approx 45^\circ$ with a razor blade and leaving them in a controlled temperature and humidity environment ($20\text{ }^\circ\text{C}$ and 80%) for a period 12 h, as illustrated in Figure 2, where ω is the deformation direction. The ratio between the storage modulus of the virgin and healed sample was used as a measure of healing efficiency, see Equation (2).

$$\epsilon = \frac{E_{\text{SH}}}{E_{\text{V}}} \times 100 \quad (2)$$

where E_{SH} and E_{V} are the storage modulus of the healed and virgin sample at the temperature and frequency considered.

Manual tests at room temperature were also performed to prove the self-healing ability. The virgin sample Poly(PEGMA-5-UPy) was cut into two pieces, and after healing, the two pieces were well-bonded, and the healed sample was strong enough to sustain stretching without damage.

Optical images attesting to the self-healing ability of this sample are shown in Figure S1, Supporting Information.

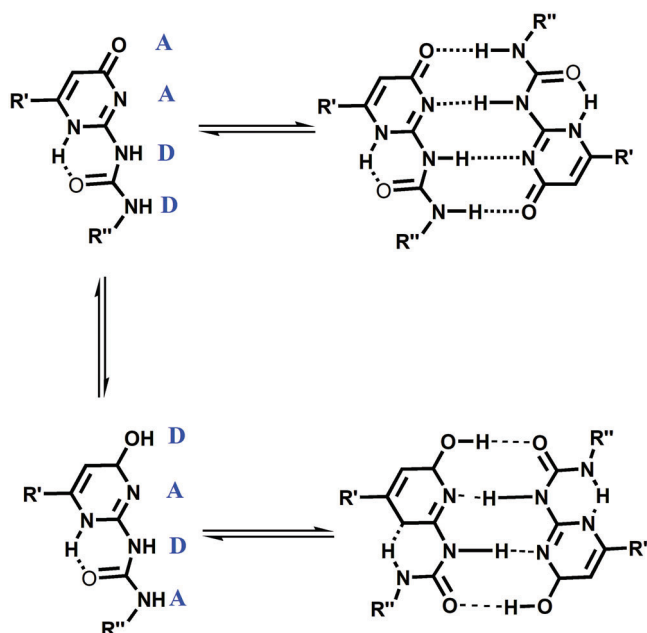


Figure 3. Tautomeric equilibrium of ureidopyrimidinones.

3. Results

3.1. Synthesis of Poly(PEGMA-co-UPy)

The Poly(PEGMA-co-UPy) copolymers were synthesized by three reaction steps, as shown in Figure 1 of the Experimental Section, following a slightly modified procedure previously reported by Chen et al.^[66]

As reported in literature by Folmer et al., in the first step, OCN-UPy was obtained by reaction of 2-amino-4-hydroxy-6-methylpyrimidine with an excess of hexamethylene diisocyanate: the nucleophilic addition of the primary amine to one of the two isocyanate groups leads to the product.^[71] The structure was proved by ¹H and ¹³C NMR analysis; thus, the protons on the nitrogens of urea moiety showed the characteristic singlets at $\delta = 11.9$ and 10.2 ppm in ¹H NMR spectrum (see Figures S2 and S3, Supporting Information). All attributions are reported in the Experimental Section. It is worth noting that the 2-amino-4-hydroxy-6-methylpyrimidine may exist as pyrimidinone and pyrimidinol and ¹³C NMR analysis confirms the coexistence of the two tautomeric forms. In fact, the signal at 164.04 ppm, attributable to carbonyl group is very broad. It is worth noting that the ureidopyrimidinones may dimerize via four hydrogen bonds in DDAA (donor–donor–acceptor–acceptor) or DADA (donor–acceptor–donor–acceptor) array in tautomeric forms of pyrimidinone and pyrimidinol (as shown in Figure 3). The introduction of electron-withdrawing substituents at the 6-position, as reported by Beijer et al., leads to the pyrimidinol tautomeric form due to the reduced stability of the enone while the hydrogen bond acceptor capability of its carbonyl group is reduced.^[62] Instead, the presence of n-alkyl substituents at the ureido group and at the 6-position stabilizes the keto tautomeric form, which is the only observed for OCN-UPy.^[62] ¹³C NMR spectrum of OCN-UPy shows

the sharp predictable signal of the carbonyl at $\delta = 173.3$ ppm, confirming the stabilization of this tautomeric form.

According to the literature procedure, the second step of synthesis of copolymers is the nucleophilic addition of the hydroxy group of 2-hydroxyethyl methacrylate (HEMA) to another isocyanate group of OCN-UPy to obtain HEMA-UPy.^[72]

¹H and ¹³C NMR spectra show predictable signals (see Experimental Section): the singlets at $\delta = 5.6$ and 6.1 ppm of the protons of the double bond on the methacrylic group in ¹H NMR and the signals at $\delta = 136.2$ and 126.1 ppm in ¹³C NMR spectrum diagnostic of the carbons of the methacrylic group confirm the formation of the product. The spectra are reported in Figures S4 and S5, Supporting Information.

The last step of the synthesis of the copolymers Poly(PEGMA-co-UPy) is achieved by free radical copolymerization of PEGMA with different amounts of the co-monomer HEMA-UPy. The formation of the copolymers was proved by ¹H and ¹³C NMR analysis and in the experimental part, are reported the attribution of all the peaks.

The signals of the double bond in ¹H and ¹³C NMR spectra disappear, confirming that the polymerization has occurred. The signals of ¹³C NMR spectra were assigned using support of DEPT experiments. The diagnostic resonances at $\delta = 13.0, 11.82, 10.03,$ and 5.85 ppm in ¹H NMR spectrum confirm the presence of the comonomer HEMA-UPy in the copolymer chains. The synthesized copolymers contain 2.5%, 5%, and 7.8% of HEMA-UPy, respectively. The comonomer concentration was calculated by integrating the peaks at 3.36 and 5.85 ppm of the ¹H NMR spectra of the products.

The homopolymer was synthesized by free radical polymerization and characterized by NMR spectroscopy.

It is worth noting that the solubility of copolymers is reduced with respect to that of homopolymer. In fact, the homopolymer Poly(PEGMA) is soluble in chloroform, whereas the copolymers Poly(PEGMA-co-UPy) are not, confirming the strong interactions among polymer chains. To overcome this criticality, the ¹H NMR spectra of the homopolymer and copolymers were performed in deuterated chloroform and tetrachloroethane, respectively.

Figures S6–S9, Supporting Information, reports the spectra of the polymer and copolymers.

The number average molecular weight (M_n) of all synthesized polymers and copolymers was determined by ¹H NMR spectroscopy analysis. The values are of the same order of magnitude as those reported in the literature by Chen et al. and are included in the range 1.5×10^5 – 2×10^5 Da.^[66]

Further characterization of Poly(PEGMA), Poly(PEGMA-5-UPy), and HEMA-UPy was carried out by FT-IR spectroscopy (see Figure 4). All the technical data about the FT-IR instrumentation have been reported in Section S1, Supporting Information.

The presence of the comonomer HEMA-UPy in the polymer chain is confirmed by the peak at 1662 cm^{-1} of the carbonyl (–CO–NH) stretching and the signal at 1590 cm^{-1} of the C=C stretching assigned to the aromatic ring, which are absent in the spectrum of Poly(PEGMA). This result is in agreement with what was observed by Zhou et al.^[65]

The C=O stretching vibration appears as a defined peak at 1728 cm^{-1} both for Poly(PEGMA) and Poly(PEGMA-5-UPy).

The homopolymer behaves as a viscous liquid, while the copolymers Poly(PEGMA-co-UPy), due to the crosslinking

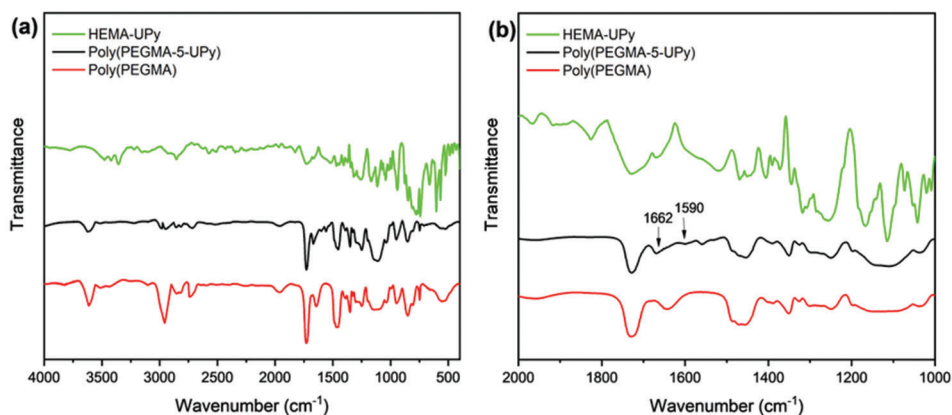


Figure 4. FT-IR spectra of HEMA-UPy, poly(PEGMA), and poly(PEGMA-5-UPy): a) range of wavenumbers 4000–400 cm^{-1} ; b) range of wavenumbers 2000–1000 cm^{-1} .

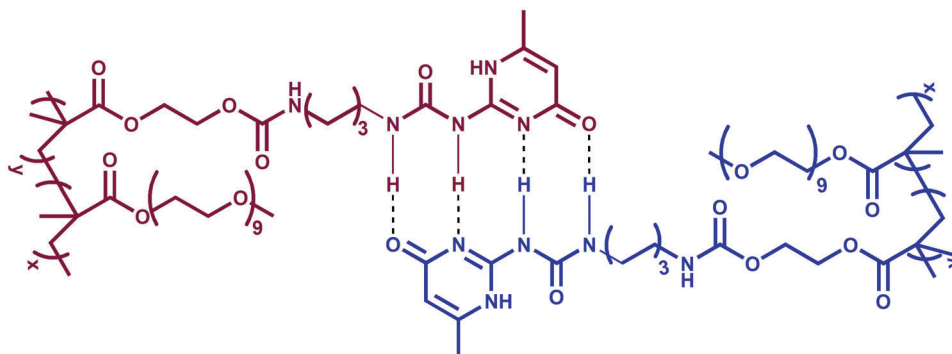


Figure 5. Quadruple hydrogen bond interactions between two Poly(PEGMA-co-UPy) chains.

generated by multiple hydrogen bonds produced by functionalities of comonomer, confer elastic features to the copolymers. Figure S10, Supporting Information shows the behavior of Poly(PEGMA-5-UPy).

The intermolecular hydrogen bonds, being reversible interactions, give the self-healing ability to these materials. The quadruple hydrogen bond interactions between two copolymer chains are depicted in **Figure 5**. The thermal properties of the polymer and copolymers and their self-healing ability were evaluated.

3.2. Thermal Analysis (TA.)

Thermal characterizations were carried out on the prepared materials to study the effect of the HEMA-UPy moiety on the thermal properties of the Poly(PEGMA) homopolymer. The effect of HEMA-UPy presence was evaluated by incorporating different percentages of HEMA-UPy into the copolymer.

Figure 6 illustrates the DSC curve for the analyzed copolymers from -90 °C to 120 °C. DSC profiles of the samples show a first thermal event (a 2nd order transition) between -65 °C and -59 °C due to the glass transition temperature (T_g), followed by an exothermic peak (crystallization temperature) with a maximum between -31 °C and -20 °C (depending on the sample composition) and the melting peak (of the crystalline fraction) with a maximum between -6 °C and -1 °C.

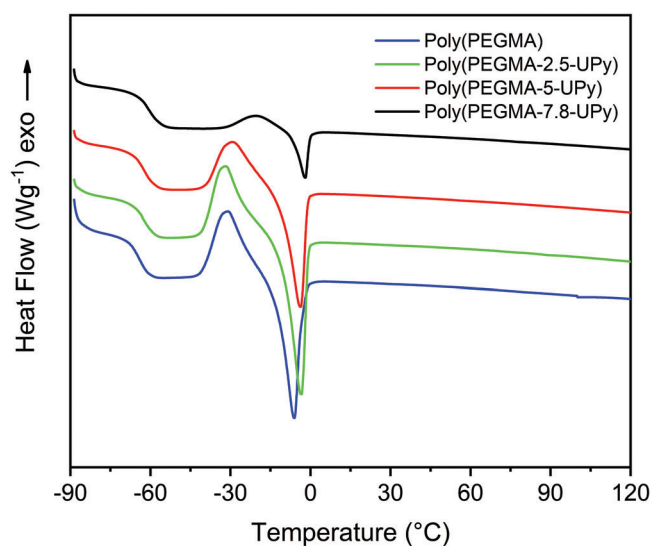


Figure 6. DSC curve of the sample from -90 °C to 120 °C.

The DSC data, shown in **Table 1**, highlight that the incorporation of HEMA-UPy unit inside the Poly(PEGMA) polymer determines a progressive enhancement of the T_g value, from -64.3 °C to -60.7 °C, and a more consistent increase both in

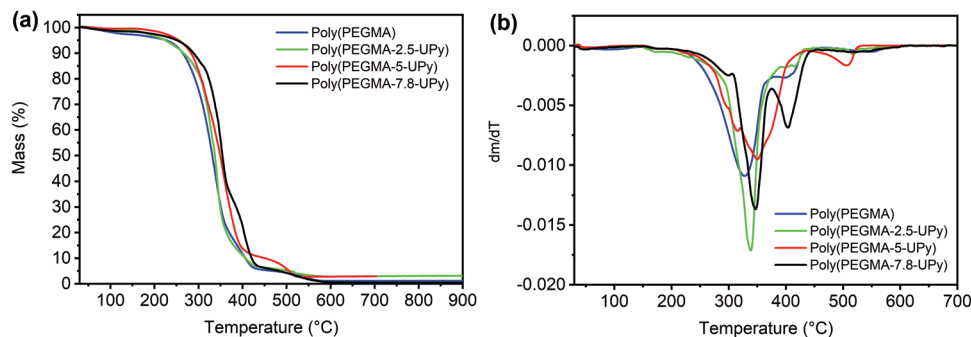


Figure 7. TGA graphs: a) mass loss curves and b) derivative mass loss curves versus temperature for the analyzed samples.

Table 1. Data of DSC analyses..

Sample	T_g [°C]	T_m [°C]	T_c [°C]	ΔH_c [Jg ⁻¹]	ΔH_m [Jg ⁻¹]	X_c
Poly(PEGMA)	-64.3	-6.06	-30.9	18.7	18.4	9.35
Poly(PEGMA-2.5-UPy)	-62.9	-3.41	-31.8	18.8	19.2	9.76
Poly(PEGMA-5-UPy)	-62.4	-3.68	-29.3	13.6	14.7	7.47
Poly(PEGMA-7.8-UPy)	-60.7	-1.89	-20.3	4.27	3.76	1.91

crystallization temperature (T_c), from -30.9 °C to -20.3 °C, and melting temperature (T_m), from -6.1 °C to -1.9 °C. A reduction in the crystallization degree (X_c) is also observed with increasing UPy amount. The increase in T_c and T_m values is more accentuated for the Poly(PEGMA-7.8-UPy) copolymer, which shows crystallization and melting temperatures higher than those of pure Poly(PEGMA) of ≈ 10 °C and 4 °C, respectively.

The effect of HEMA-UPy units on the T_g of the resulting material was also observed by other authors. In fact, this result is in agreement with what was reported in literature, where it was observed that the T_g of Poly(PEGMA)-based copolymers decreases as the Poly(PEGMA) content increases.^[65,73,74] This behavior was ascribed to the flexibility of the polymer affected by the presence of HEMA-UPy units, which are able to increase intermolecular interactions based on multiple hydrogen bonding, well depicted in Figure 5.^[64,65]

In addition, the enhancement in T_c and T_m values was expected due to the cumulative effect of hydrogen bonds. In fact, for the crystallization and melting thermal events to occur, the material must reach higher temperatures capable of breaking the strong intermolecular interactions, which most probably act as crosslinkers between the various polymeric chains. Furthermore, the progressive decrease in ΔH_c and ΔH_m values as the amount of HEMA-UPy moiety increases is due to the occurrence that the copolymerization of HEMA-UPy with PEGMA can cause disruption in the order of the crystalline PEGMA and this results in a lower crystallinity of the samples. In addition, the supramolecular interactions may hinder the crystallization process, making the polymer more amorphous and causing a consequent decrease of X_c values.^[61]

Figure 7 illustrates the profiles of the mass loss (see Figure 7a) and derivative mass loss (see Figure 7b) curves, for the characterized copolymers. All the analyzed materials show a thermal degradation profile characterized by two main stages of decomposition, the first between 300 °C and 400 °C and the second one

Table 2. TGA data..

Sample	$T_{d5\%}$ [°C]	$T_{d50\%}$ [°C]	Residue at 900 °C
Poly(PEGMA)	227.2	331.3	1.7
Poly(PEGMA-2.5-UPy)	225.2	337.1	3.5
Poly(PEGMA-5-UPy)	255.8	349.2	2.9
Poly(PEGMA-7.8-UPy)	251.7	354.3	1.50

over 400 °C. The TGA and DTGA curves clearly show how the presence of the HEMA-UPy fraction, in the percentages of 5 wt% and 7.8 wt% (see red and black curves in Figure 7a,b), determines an increase in the thermal stability of the Poly(PEGMA), conferring to the Poly(PEGMA-5-UPy) and Poly(PEGMA-7.8-UPy) copolymers values of $T_{d5\%}$ (temperature corresponding to a mass loss of 5 wt%), illustrated in Table 2, higher than ≈ 30 °C, with respect to the Poly(PEGMA) and Poly(PEGMA-2.5-UPy) samples. A similar trend is also observed for the $T_{d50\%}$ value (temperature corresponding to a mass loss of 50 wt%), which increases by ≈ 20 °C for the Poly(PEGMA-7.8-UPy) copolymer (see Table 2). These results evidence that the thermal stability of Poly(PEGMA) can be improved by HEMA-UPy units, as already observed for other thermoplastic matrices, supporting the hypothesis that the strong intermolecular interactions, based on the hydrogen bonds, act as crosslinkers between the Poly(PEGMA) chains, increasing the thermal stability of the materials.^[75] Furthermore, the combined results of DSC and TGA analyses highlight the cumulative effect of H-bonds, most evident in the sample containing a more significant amount of HEMA-UPy moiety.

3.3. Self-Healing Efficiency Evaluation

The healing efficiency was investigated only for sample Poly(PEGMA-5-UPy). This composition was selected because TA demonstrated that the presence of 5 wt% of HEMA-UPy, incorporated in Poly(PEGMA) matrix, is enough to get a material having strong intermolecular interactions, without excessively altering its flexibility and making it the best candidate for preparing self-healing multifunctional composites. Figure 8 shows the variation of storage modulus of the virgin sample (see continuous curves in Figure 8a) and of storage modulus of the healed sample (see dashed curves in Figure 8a), as a function of temperature and frequencies. The healing efficiency, calculated by the ratio of the storage moduli according to Equation (2) and showed

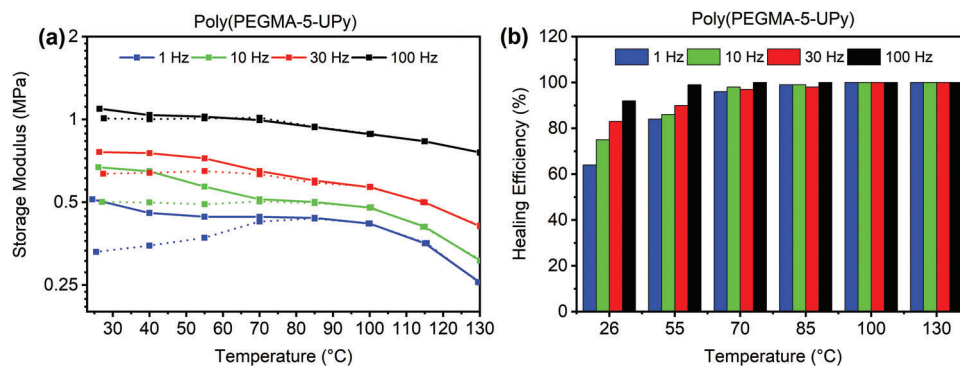


Figure 8. a) Storage modulus versus temperature at different values of frequency, for the virgin sample (continuous curve) and for the healed sample (dashed curve); b) histogram showing the healing efficiency at different values of frequency and temperature.

in the histogram of Figure 8a,b, evidences that the storage modulus increases with increasing frequency. Furthermore, for the same frequency, all the virgin samples are in the rubbery plateau region (the modulus is almost constant) up to 100 °C. Beyond this value of temperature, the modulus decreases with increasing the temperature. As expected, the transition temperature between the different trends of the elastic modulus shifts at higher values by increasing the frequency. The healed sample (dashed curves in Figure 8a) shows an initial increase in the storage modulus up to ≈ 70 °C followed by a plateau region before a progressive decrease. At temperatures higher than 100 °C, the curves of the virgin and healed samples overlap almost perfectly. This is a clear indication of a complete recovery of the mechanical properties with the temperature. This behavior is due to the occurrence that higher temperature values determine an increase in molecular mobility that increases the recovery rate of the samples. Furthermore, for temperatures lower than 70 °C, the recovery rate seems to increase by increasing the frequency. Probably, this behavior is due to the heat developed inside the sample solicited at high values of frequency; and therefore, due to its viscoelastic behavior (see Figure S11, Supporting Information). The heat generated by the friction between the molecules determines a local increase in the temperatures, which increases the recovery rate. This effect becomes negligible when the temperature of the test is already high enough. Therefore, at high temperatures, the recovery rate is dominated only by the temperature imposed during the DMA test. Starting by the value of recovery rate of 64% at 26 °C, a continuous increase in the recovery rate is detected up to 70 °C. Considering that the sample is kept to heal at room temperature, it is most likely that the increase in the recovery rate is due to additional healing determined by the higher temperature (with respect to the room temperature) employed during the DMA test. Beyond the value of 70 °C, no further healing occurs because the samples have already reached the maximum value of recovery rate (100%).

The healing behavior of thermoplastic polymers under dynamic mechanical solicitations seems to exhibit a similar behavior. The same methodology was applied to evaluate the healing efficiency of a biodegradable thermoplastic polymer containing solubilized Murexide (M) salts in a commercial biodegradable vinyl alcohol copolymer (HVA). The healing efficiency was evaluated by the recovery of the storage modulus as a function of the temperature at different values of tensile deformation frequency. The

measurements performed on the polymeric system with varying amounts of M manifested a healing efficiency increase as the frequency increased. The dependence of the healing efficiency on the frequency was lost at temperatures equal to/or higher than 90 °C.^[61]

4. Conclusion

In this work, a supramolecular elastomer Poly(PEGMA-co-UPy) was synthesized by incorporating different percentages of HEMA-UPy units in the Poly(PEGMA) matrix to confer the auto-repair ability to the polymeric matrix. This material, previously synthesized and characterized in the literature, is analyzed here as model system. The TA has proven to be an effective methodology to investigate the presence of supramolecular interactions together with their cumulative effects. Furthermore, a new and innovative approach, based on the DMA investigation, has been proposed to obtain quantitative results on the healing efficiency at different temperatures and in dynamic conditions. DSC analysis has shown that, by increasing the amount of HEMA-UPy, glass transition, melting, and crystallization temperatures increase; thus, determining a simultaneous decrease of crystallization degree. TGA measurements highlight that the thermal stability of the samples considerably improves with increasing the percentage of HEMA-UPy. DMA tests have been employed to assess the auto-repair ability of the samples under dynamic stresses characterized by different frequency values. They confirm the excellent self-healing ability of Poly(PEGMA-5-UPy) copolymer, providing additional information on the self-healing behavior at different values of frequency and temperature. The mechanical recovery is dependent on the temperature up to a defined value of temperature. High temperatures allow faster healing, with an almost complete recovery already at the temperature of 70 °C. These results demonstrate the key role of HEMA-UPy moiety in enhancing intermolecular interaction between the polymeric chains due to multiple hydrogen bonding. These interactions can be favored by suitable values of temperature.

Supporting Information

Supporting Information is available from the Wiley Online Library or from the author.

Acknowledgements

The authors thank Patrizia Oliva of the Department of Chemistry and Biology of the University of Salerno for the technical assistance.

Conflict of Interest

The authors declare no conflict of interest.

Data Availability Statement

The data that support the findings of this study are available from the corresponding author upon reasonable request.

Keywords

hydrogen bonds, self-healing materials, supramolecular chemistry

Received: July 28, 2022

Revised: October 7, 2022

Published online: November 11, 2022

- [1] E. B. Murphy, F. Wudl, *Prog. Polym. Sci.* **2010**, *35*, 223.
- [2] Y. Yang, M. W. Urban, *Chem. Soc. Rev.* **2013**, *42*, 7446.
- [3] B. J. Blaiszik, S. L. B. Kramer, S. C. Olugebefola, J. S. Moore, N. R. Sottos, S. R. White, *Annu. Rev. Mater. Res.* **2010**, *40*, 179.
- [4] S. R. White, N. R. Sottos, P. H. Geubelle, J. S. Moore, M. R. Kessler, S. R. Sriram, E. N. Brown, S. Viswanathan, *Nature* **2001**, *409*, 794.
- [5] S. H. Cho, H. M. Andersson, S. R. White, N. R. Sottos, P. V. Braun, *Adv. Mater.* **2006**, *18*, 997.
- [6] M. M. Caruso, B. J. Blaiszik, H. Jin, S. R. Schelkopf, D. S. Stradley, N. R. Sottos, S. R. White, J. S. Moore, *ACS Appl. Mater. Interfaces* **2010**, *2*, 1195.
- [7] Y. C. Yuan, M. Z. Rong, M. Q. Zhang, *Polymer* **2008**, *49*, 2531.
- [8] J. D. Rule, E. N. Brown, N. R. Sottos, S. R. White, J. S. Moore, *Adv. Mater.* **2005**, *17*, 205.
- [9] L. Guadagno, M. Raimondo, C. Naddeo, P. Longo, A. Mariconda, *Polym. Eng. Sci.* **2014**, *54*, 777.
- [10] K. S. Toohey, N. R. Sottos, J. A. Lewis, J. S. Moore, S. R. White, *Nat. Mater.* **2007**, *6*, 581.
- [11] K. S. Toohey, C. J. Hansen, J. A. Lewis, S. R. White, N. R. Sottos, *Adv. Funct. Mater.* **2009**, *19*, 1399.
- [12] P. Longo, A. Mariconda, E. Calabrese, M. Raimondo, C. Naddeo, L. Vertuccio, S. Russo, G. Iannuzzo, L. Guadagno, *J. Ind. Eng. Chem.* **2017**, *54*, 234.
- [13] E. Calabrese, P. Longo, C. Naddeo, A. Mariconda, L. Vertuccio, M. Raimondo, L. Guadagno, *Int. J. Struct. Integr.* **2018**, *9*, 723.
- [14] L. Guadagno, P. Longo, M. Raimondo, C. Naddeo, A. Mariconda, A. Sorrentino, V. Vittoria, G. Iannuzzo, S. Russo, *J. Polym. Sci., Part B: Polym. Phys.* **2010**, *48*, 2413.
- [15] J. Van Stappen, T. Bultreys, F. A. Gilibert, X. K. D. Hillewaere, D. G. Gómez, K. Van Tittelboom, J. Dhaene, N. De Belie, W. Van Paeppegem, F. E. Du Prez, V. Cnudde, *Mater. Charact.* **2016**, *119*, 99.
- [16] S. Utrera-Barrios, R. Verdejo, M. A. López-Manchado, M. Hernández Santana, *Mater. Horiz.* **2020**, *7*, 2882.
- [17] M. Lu, Y. Song, Q. Zheng, W. Wang, *J. Polym. Sci.* **2022**, *60*, 2855.
- [18] X. X. Chen, M. A. Dam, K. Ono, A. Mal, H. B. Shen, R. N. Steven, K. Sheran, F. Wudl, *Science* **2002**, *295*, 698.
- [19] X. Chen, F. Wudl, A. K. Mal, H. Shen, S. R. Nutt, *Macromolecules* **2003**, *36*, 1802.
- [20] T. A. Plaisted, S. Nemat-Nasser, *Acta Mater.* **2007**, *55*, 5684.
- [21] Jong Se Park, K. Takahashi, Z. Guo, Y. Wang, E. d Bolanos, C. Hamann-Schaffner, E. Murphy, F. Wudl, H. T. Hahn, *J. Compos. Mater.* **2008**, *42*, 2869.
- [22] J. S. Park, H. S. Kim, H. Thomas Hahn, *Compos. Sci. Technol.* **2009**, *69*, 1082.
- [23] E. B. Murphy, E. d Bolanos, C. Schaffner-Hamann, F. Wudl, S. R. Nutt, M. L. Auad, *Macromolecules* **2008**, *41*, 5203.
- [24] A. M. Peterson, R. E. Jensen, G. R. Palmese, *Appl. Mater. Interfaces* **2009**, *1*, 992.
- [25] S. Jung, J. K. Oh, *Mater Today Commun* **2017**, *13*, 241.
- [26] D. Wang, J. Z. S. Chen, Z. Zhang, *Mater. Today Commun.* **2020**, *23*, 101138.
- [27] A. M. Peterson, R. E. Jensen, G. R. Palmese, *ACS Appl. Mater. Interfaces* **2010**, *2*, 1141.
- [28] P. A. Pratama, M. Sharifi, A. M. Peterson, G. R. Palmese, *ACS Appl. Mater. Interfaces* **2013**, *5*, 12425.
- [29] D. Ehrhardt, J. Mangialetto, J. Bertouille, K. Van Durme, B. Van Mele, N. Van Den Brande, *Polymers* **2020**, *12*, 2543.
- [30] S. J. Kalista, T. C. Ward, Z. Oyetunji, *Mech. Adv. Mater. Struct.* **2007**, *14*, 391.
- [31] S. J. Kalista, T. C. Ward, *J. R. Soc., Interface* **2007**, *4*, 405.
- [32] R. J. Varley, S. Van Der Zwaag, *Acta Mater.* **2008**, *56*, 5737.
- [33] R. John Varley, S. Van Der Zwaag, *Polym. Test.* **2008**, *27*, 11.
- [34] P. Cordier, F. Tournilhac, C. Soulie-Ziakovic, L. Leibler, *Nature* **2008**, *451*, 977.
- [35] D. Montarnal, F. Tournilhac, M. Hidalgo, J.-L. Couturier, L. Leibler, *J. Am. Chem. Soc.* **2009**, *131*, 7966.
- [36] L. Vertuccio, L. Guadagno, G. Spinelli, P. Lamberti, M. Zarrelli, S. Russo, G. Iannuzzo, *Composites, Part B* **2018**, *147*, 42.
- [37] A. M. Wemyss, C. Bowen, C. Plesse, C. Vancaeyzeele, G. T. M. Nguyen, F. Vidal, C. Wan, *Mater. Sci. Eng., C* **2020**, *141*, 100561.
- [38] M. Zhu, J. Liu, L. Gan, M. Long, *Eur. Polym. J.* **2020**, *129*, 109651.
- [39] V. K. Thakur, M. R. Kessler, *Polymer* **2015**, *69*, 369.
- [40] L. Guadagno, A. Sorrentino, P. Delprat, L. Vertuccio, *Nanomaterials* **2020**, *10*, 2285.
- [41] M. Raimondo, C. Naddeo, L. Vertuccio, L. Bonnaud, P. Dubois, W. H. Binder, A. Sorrentino, L. Guadagno, *Nanotechnology* **2020**, *31*, 225708.
- [42] L. Guadagno, L. Vertuccio, C. Naddeo, E. Calabrese, G. Barra, M. Raimondo, A. Sorrentino, W. H. Binder, P. Michael, S. Rana, *Polymers* **2019**, *11*, 903.
- [43] L. Guadagno, A. Mariconda, A. Agovino, M. Raimondo, P. Longo, *Composites, Part B* **2017**, *116*, 352.
- [44] L. Guadagno, L. Vertuccio, C. Naddeo, E. Calabrese, G. Barra, M. Raimondo, A. Sorrentino, W. H. Binder, P. Michael, S. Rana, *Composites, Part B* **2019**, *157*, 1.
- [45] A. Kausar, *J. Plast. Film Sheeting* **2021**, *37*, 160.
- [46] L. Guadagno, C. Naddeo, M. Raimondo, G. Barra, L. Vertuccio, A. Sorrentino, W. H. Binder, M. Kadlec, *Composites, Part B* **2017**, *128*, 30.
- [47] M. Raimondo, E. Calabrese, W. H. Binder, P. Michael, S. Rana, L. Guadagno, *Polymers* **2021**, *13*, 1401.
- [48] D. A. Simon, E. Bischoff, G. G. Buonocore, P. Cerruti, M. G. Raucchi, H. Xia, H. S. Schrekker, M. Lavorgna, L. Ambrosio, R. S. Mauler, *Mater. Des.* **2017**, *134*, 103.
- [49] L. Guadagno, L. Vertuccio, C. Naddeo, G. Barra, M. Raimondo, A. Sorrentino, W. H. Binder, P. Michael, S. Rana, E. Calabrese, *Mater. Today: Proc.* **2021**, *34*, 243.
- [50] C. Wang, N. Liu, R. Allen, J. B.-H. Tok, Y. Wu, F. Zhang, Y. Chen, Z. Bao, *Adv. Mater.* **2013**, *25*, 5785.
- [51] B. C.-K. Tee, C. Wang, R. Allen, Z. Bao, *Nat. Nanotechnol.* **2012**, *7*, 825.
- [52] J. Liu, G. Song, C. He, H. Wang, *Macromol. Rapid Commun.* **2013**, *34*, 1002.

- [53] N. Yan, F. Capezzuto, G. G. Buonocore, M. Lavorgna, H. Xia, L. Ambrosio, *ACS Appl. Mater. Interfaces* **2015**, *7*, 22678.
- [54] K. Z. Donato, M. Lavorgna, R. K. Donato, M. G. Raucci, G. G. Buonocore, L. Ambrosio, H. S. Schrekker, R. S. Mauler, *ACS Sustainable Chem. Eng.* **2017**, *5*, 1094.
- [55] Y.-L. Wang, M. Stanzione, H. Xia, G. G. Buonocore, E. Fortunati, S. Kaciulis, M. Lavorgna, *Compos. Sci. Technol.* **2020**, *200*, 108458.
- [56] S. Manzetti, J.-C. P. Gabriel, *Int. Nano Lett.* **2019**, *9*, 31.
- [57] R. Peng, Y. Wang, W. Tang, Y. Yang, X. Xie, *Polymers* **2013**, *5*, 847.
- [58] J. Wang, H. Chu, Y. Li, *ACS Nano* **2008**, *2*, 2540.
- [59] F. Fabrício, A. A. Silva, B. G. Soares, *Polym. Eng. Sci.* **2018**, *58*, 1689.
- [60] L. Guadagno, L. Vertuccio, G. Barra, C. Naddeo, A. Sorrentino, M. Lavorgna, M. Raimondo, E. Calabrese, *Polymer* **2021**, *223*, 123718.
- [61] L. Guadagno, M. Raimondo, M. Catauro, A. Sorrentino, E. Calabrese, *J. Therm. Anal. Calorim.* **2022**, *147*, 5463.
- [62] F. H. Beijer, R. P. Sijbesma, H. Kooijman, A. L. Spek, E. W. Meijer, *J. Am. Chem. Soc.* **1998**, *120*, 6761.
- [63] A. Faghihnejad, K. E. Feldman, J. Yu, M. V. Tirrell, J. N. Israelachvili, C. J. Hawker, E. J. Kramer, H. Zeng, *Adv. Funct. Mater.* **2014**, *24*, 2322.
- [64] D. Zhu, Q. Ye, X. Lu, Q. Lu, *Polym. Chem.* **2015**, *6*, 5086.
- [65] B. Zhou, D. He, J. Hu, Y. Ye, H. Peng, X. Zhou, X. Xie, Z. Xue, *J. Mater. Chem. A* **2018**, *6*, 11725.
- [66] J. Chen, J. Liu, T. Thundat, H. Zeng, *ACS Appl. Mater. Interfaces* **2019**, *11*, 18720.
- [67] S. Sundararajan, A. B. Samui, P. S. Kulkarni, *React. Funct. Polym.* **2018**, *130*, 43.
- [68] Y. Li, R. Liu, Y. Huang, *J. Appl. Polym. Sci.* **2008**, *110*, 1797.
- [69] U. Gaur, B. Wunderlich, *J. Phys. Chem. Ref. Data* **1981**, *10*, 1001.
- [70] K. Pielichowska, J. Bieda, P. Szatkowski, *Renew. Energy* **2016**, *91*, 456.
- [71] B. J. B. Folmer, R. P. Sijbesma, R. M. Versteegen, J. A. J. Van Der Rijt, E. W. Meijer, *Adv. Mater.* **2000**, *12*, 874.
- [72] J. Chen, B. Yan, X. Wang, Q. Huang, T. Thundat, H. Zeng, *Polym. Chem.* **2017**, *8*, 3066.
- [73] C.-Y. Park, B.-J. Chang, J.-H. Kim, Y. M. Lee, *J. Membr. Sci.* **2019**, *587*, 117167.
- [74] Y. Matsumura, T. Shiraiwa, T. Hayasaka, S. Yoshida, B. Ochiai, *J. Electrochem. Soc.* **2018**, *165*, B3119.
- [75] Z. Wang, Y. Ding, J. Wang, *Nanomaterials* **2019**, *9*, 1397.